

Characterization of 2004 Indian Ocean Tsunami induced deposits along the Chennai coast using magnetic and geochemical techniques

S. Veerasingam^{1*} & R. Venkatachalapathy²

¹CSIR-National Institute of Oceanography, Dona Paula, Goa-403004, India

²Faculty of Marine Sciences, Annamalai University, Parangipettai, Tamil Nadu – 608 502, India

*[Email: veerasingams@nio.org]

Received 15 August 2013; revised 16 October 2013

Present study is the applicability of rock magnetic techniques, coupled with geochemical (SiO₂, Al₂O₃, Fe₂O₃, CaO, MgO, K₂O, P₂O₅, and MnO) and texture size measurements, as a proxy tool to identify tsunami induced deposits in the core sediments from the Chennai coast, India. Down core profiles of mass specific magnetic susceptibility (χ), χ_{ARM} and SIRM are similar in all sediment cores, and reflect changes in the detrital component mineralogy which is largely influenced by the tsunami event. To identify the connection between the tsunami deposit and different sedimentologic units present in the study area, textural, geochemical and rock magnetic data were processed by multivariate statistical analyses.

[**Keywords:** Tsunami deposit, texture size, geochemistry, rock-magnetism, multivariate statistics.]

Introduction

Tsunami is one of the most serious natural hazards known to human and has been responsible for tremendous human and economic loss. Following the recent tsunamis in Indonesia (2004), Chile (2010) and Japan (2011), the risks associated with tsunamis have come into focus. Most tsunamis occur in the marine region and are coupled with huge earthquakes¹. Since the Indian Ocean Tsunami (IOT) in 2004, by far the largest natural catastrophe in human history, the worldwide scientific community deployed numerous investigations of tsunami deposits to assess tsunami impact. The 26 December 2004 tsunami event devastated several major coastlines in South Asia, including the Tamil Nadu coast, India. The IOT was generated by one of the largest earthquakes of the past 100 years, and its epicentre located near 3.3°N and 95.95°E with a magnitude of 9.0 and focal depth of 10 km².

Tsunami waves have sufficiently high velocities and bed shear stresses to suspend and transport large quantities of sediment³. Modern studies of tsunami are often troubled by the lack of information on the frequency and magnitude of past events. In many cases, the unique information that can be used consists of historical records. Therefore, it is often difficult to provide a quantitative assessment of tsunami risk since historical data sets typically cover only a relatively short period. Identification of past

tsunamis is crucial for risk assessment studies, especially in areas where the historical record is limited or missing⁴.

Reconstruction of long-term frequency of paleo-tsunami is still hard to reach due to the weak conservation of the tsunami deposits in the geological record and to the difficulty in distinguishing them from storm deposits, which have similar depositional mechanisms⁵. Various aspects of 2004 IOT onshore deposits on the east coast of India were reported by several researchers⁶⁻¹⁵. In this study, we couple rock magnetic and geochemical proxies, using both destructive and non-destructive methods to carry out high-resolution characterization of the Indian Ocean Tsunami deposits along the Chennai coast.

Materials and Methods

The coastal region of southeast coast of India was affected in a devastating manner during the 2004 Indian Ocean Tsunami where three large waves hit the Indian coast 3h after the major earthquake. The Chennai metropolitan city is located on the southeast coast of India. Two major rivers meander through Chennai, the Coovum River through the centre and the Adayar River to the south. Two sediment cores (C and A) were collected from the mouth of Coovum and Adayar estuaries using a hand operated corer on July 2008 (Fig.1). Soon after collection, the cores

were sectioned into 2.5 cm intervals using a plastic knife from the surface. The sub-samples were sealed in clean plastic bags, labelled and stored in icebox till the completion of laboratory analyses.

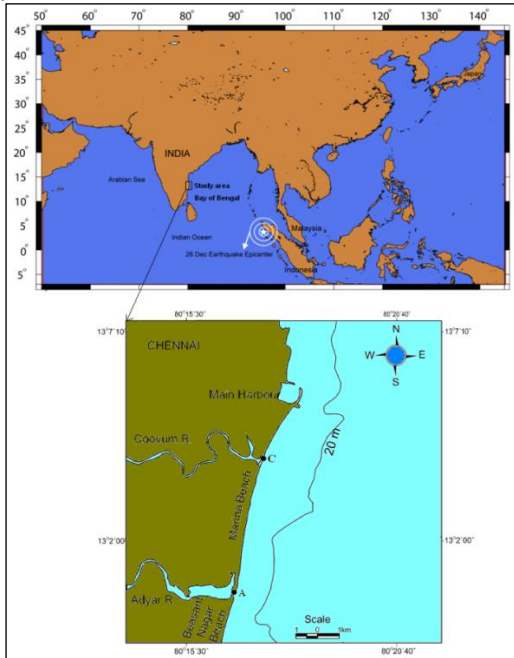


Fig. 1—Study area and sampling locations

The sediment texture such as sand, silt and clay were measured following the procedure of¹⁶. The samples were oven-dried ($\sim 100^\circ$), powdered in an agate mortar and analysed for elements such as SiO_2 , Al_2O_3 , Fe_2O_3 , CaO , MgO , K_2O , P_2O_5 , and MnO on powdered and pressed pellets with a Thermo Scientific Niton XL2 X ray fluorescence spectrometer. Dried sediment samples packed in 10 ml polystyrene pots before being subject to the rock magnetic measurements. Magnetic susceptibility (χ) measurements were carried out using a Bartington MS-2 magnetic susceptibility meter (with alternating current magnetic field amplitude of 80 A/m) linked to an MS2B dual-frequency sensor (0.47 and 4.7 kHz). The average of five measurements is presented as mass specific values in $10^{-8} \text{ m}^3\text{kg}^{-1}$. The frequency dependence of susceptibility (χ_{fd}) is calculated using the following formula:

$$\chi_{fd}\% = [(\chi_{lf} - \chi_{hf}) / \chi_{lf}] \times 100$$

where, χ_{lf} and χ_{hf} are the low and high frequency mass specific magnetic susceptibilities. Anhysteretic remanent magnetization (ARM) was induced in samples using Molspin alternating-field demagnetizers, with 100 mT peak alternating field and a 0.05 mT steady field. ARM is expressed here as anhysteretic susceptibility (χ_{ARM}

= ARM/ strength of the biasing field). ARM and all subsequent remanences was measured using Molspin fluxgate spinner magnetometer. Isothermal Remanent Magnetization (IRM) is the remanent magnetization acquired by a sample after exposure to, and removal from, a steady (DC) magnetic field¹⁷. IRM was measured for forward fields of 20mT, 1T and 2T and a reverse field of 20mT, 30mT, 40mT, 60mT, 80mT, 100mT and 300mT. IRM_{2T} is hereafter, referred to as the Saturation Isothermal Remanent Magnetization (SIRM). χ_{ARM}/χ_s , SIRM/ χ_s , Soft IRM (= SIRM - IRM_{-30mT}) and Hard IRM (= SIRM - IRM_{-300mT}) were measured using forward DC fields. S-ratio (= IRM₋₃₀₀ / SIRM, being IRM₋₃₀₀ the acquired IRM at a backfield of 300mT) are also calculated from IRM measurement, using backfield once the SIRM was reached. The correlation analysis was carried out to find the relationships among the sediment texture, mineral, geochemical and rock-magnetic parameters in sediments.

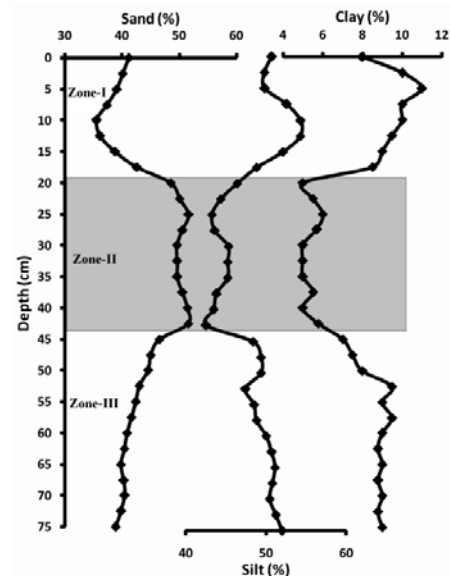


Fig. 2a—Down core variations of sand, silt and clay in sediment core (A) from Adayar estuary.

Results and Discussion

Sediment texture and geochemistry

Textural parameters of sediment reflect the energy conditions of the depositional environment. The down core profiles of texture sizes for Adayar and Coovum estuarine sediment cores are given in Fig.2a, b.

The average values of sand, silt and clay contents in 'A' core are 43.8%, 48.6% and 7.8%, while in 'C' core are 42.9%, 49.4% and 9.1%, respectively. Texture size analysis of both sediment cores indicates three zones namely zone

I, II and III. The mean sand content in the 'A' and 'C' cores in the zone II are 50.4% and 78.4% respectively. The sandy nature of the zone II sediment samples confirms that it is associated with the erosion/depositional features from the land/beach due to the high-energy waves and intense current action that hit the coast.

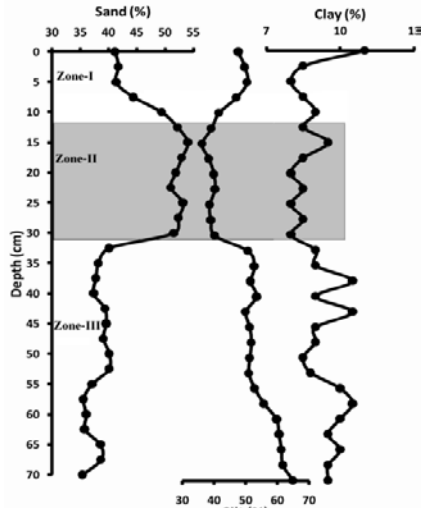


Fig. 2b—Down core variations of sand, silt and clay in sediment core (B) from Coovum estuary.

The geochemical process in the coastal region and the effect of tsunami waves on the overall distribution process is evaluated using vertical distribution of geochemical elements. The vertical distribution of major geochemical elements in sediment cores is given in Fig. 3a and 3b. Zone I and III present similar geochemical values while the zone II is characterized by an abrupt shift of geochemistry in both sediment cores.

The high values of SiO_2 (A: 49.4 – 51.5%; C: 51 – 52.5%) and K_2O (A: 1.99 – 2.31%; C: 1.83 – 1.99%) and low values of Al_2O_3 (A: 3.53 – 3.64%; C: 3.45 – 3.57%), Fe_2O_3 (A: 0.748 – 0.759%; C: 0.731 – 0.739%), CaO (A: 1.87 – 2.69%; C: 2.36 – 2.42%), MgO (A: 0.61 – 0.97%; C: 1.07 – 1.10%), P_2O_5 (A: 0.0767 – 0.0773%; C: 0.0767 – 0.0768%) and MnO (A: 0.11 – 0.15%; C: 0.067 – 0.108%) were obtained in zone II. Geochemical analysis indicates that zone II have higher amount of Al rich silt/clay than zones I and III. These differences could reflect changes in the source, energy of the depositional environment or transport mechanisms. The distribution pattern of MgO , K_2O and P_2O_5 indicates marginal loss in concentration throughout the sediment cores. But the concentration of CaO indicates a loss of half of the content in Zones I and III than Zone II suggesting rapid transportation/deposition.

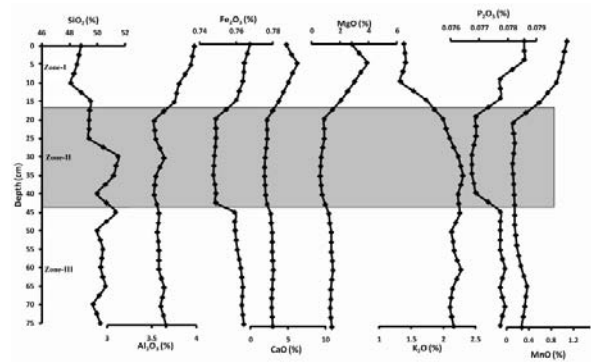


Fig. 3a—Vertical distribution of major elements in sediment core (A) from Adayar estuary

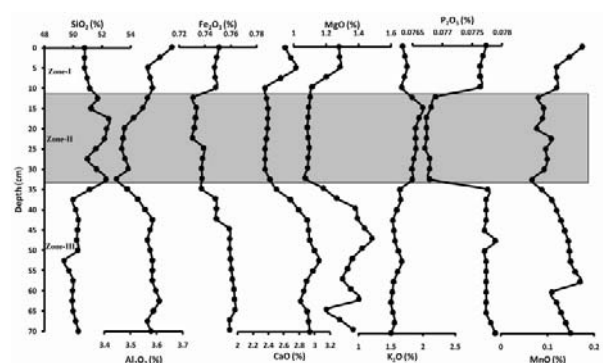


Fig. 3b—Vertical distribution of major elements in sediment core (C) from Coovum estuary.

Magnetic concentration dependent parameters

Magnetic susceptibility (χ) generally reflects physical changes in the depositional environment in relation to climate and environmental changes. χ reflects the bulk concentration of magnetisable material down-core, independently of the grain size of the magnetic components. Saturation Isothermal Remanent Magnetisation (SIRM) mainly reflects the combined concentration of ferrimagnetic (i.e. magnetite and maghemite) and imperfect anti-ferromagnetic (i.e. hematite and goethite) minerals. χ_{ARM} is particularly sensitive to the concentration of stable single domain ferrimagnetic grains. Data of concentration dependent magnetic parameters (χ , SIRM, and χ_{ARM}) for A and C are shown in Fig. 4a and 4b. The ranges of magnetic susceptibility for A and C sediment cores are $12 - 47.9 \times 10^{-8} \text{ m}^3 \text{ kg}^{-1}$ (Average $28.7 \times 10^{-8} \text{ m}^3 \text{ kg}^{-1}$) and $20.7 - 52 \times 10^{-8} \text{ m}^3 \text{ kg}^{-1}$ (Average $33.4 \times 10^{-8} \text{ m}^3 \text{ kg}^{-1}$) respectively. Values of SIRM vary between $134.13 - 240.64 \times 10^{-5} \text{ Am}^2 \text{ kg}^{-1}$ (Average $188.72 \times 10^{-5} \text{ Am}^2 \text{ kg}^{-1}$) and $94.64 - 196.32 \times 10^{-5} \text{ Am}^2 \text{ kg}^{-1}$ (Average $138.23 \times 10^{-5} \text{ Am}^2 \text{ kg}^{-1}$) respectively. Likewise, χ_{ARM} values for A and C sediment cores varied from $0.11-0.26 \times 10^{-5} \text{ m}^3 \text{ kg}^{-1}$ (Average $0.20 \times 10^{-5} \text{ m}^3 \text{ kg}^{-1}$) and $0.02 - 0.21 \times 10^{-5} \text{ m}^3 \text{ kg}^{-1}$ (0.11×10^{-5}

$5\text{ m}^3\text{kg}^{-1}$) respectively. Zone I and III show similar magnetic susceptibility, SIRM, and χ_{ARM} values while the tsunami deposit (Zone II) is characterized by a sudden decrease of χ (A: $\sim 17.7 \times 10^{-8} \text{ m}^3 \text{ kg}^{-1}$; C: $\sim 25.6 \times 10^{-8} \text{ m}^3 \text{ kg}^{-1}$), SIRM (A: $\sim 155.69 \times 10^{-5} \text{ Am}^2 \text{ kg}^{-1}$; C: $\sim 118.4 \times 10^{-5} \text{ Am}^2 \text{ kg}^{-1}$) and χ_{ARM} (A: $\sim 0.15 \times 10^{-5} \text{ m}^3\text{kg}^{-1}$; C: $\sim 0.05 \times 10^{-5} \text{ m}^3\text{kg}^{-1}$) indicative of a very low contribution of ferrimagnetic minerals or the high contribution of paramagnetic/diamagnetic minerals into the sediment matrix. In zone I and III, χ , χ_{ARM} and SIRM values show higher concentration of ferrimagnetic oxides.

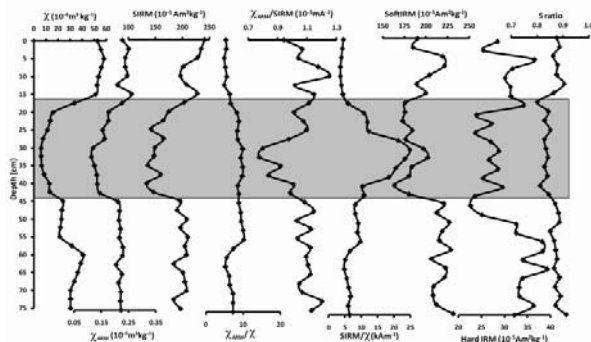


Fig. 4a—Vertical distribution of rock magnetic parameters in sediment core (A) from Adayar estuary.

Magnetic grain size distribution

The four general magnetic domain structures are stable single domain (SSD), pseudo-single domain (PSD), multi-domain (MD) and super-paramagnetic (SP). The domain structure plays an important role in the magnetic properties of ferro- or ferrimagnetic minerals. The temporal trends of magnetic grain size dependent parameters are shown in Figs 4a and 4b. The quotients of $\chi_{\text{ARM}}/\text{SIRM}$ and SIRM/χ are used to highlight variations in grain size trends within magnetic grain assemblies. Peters and Dekkers¹⁸ pointed out that χ_{ARM}/χ values decrease with increasing magnetite grains sizes. χ_{ARM}/χ is sensitive to the finer magnetic grain sizes (above the threshold for stable SD behaviour), while $\chi_{\text{ARM}}/\text{SIRM}$ is sensitive to the coarser (PSD to MD) grain sizes¹⁹. The $\chi_{\text{ARM}}/\text{SIRM}$ ratio is related to the magnetic grain size: for magnetite, values greater than about $1 \times 10^{-3} \text{ mA}^{-1}$ are indicative of grains close to stable single domain size²⁰. The grain size parameters show similar SD nature while χ values increase significantly together with SIRM and χ_{ARM} values suggesting that it may correspond to a change in magnetic particle content rather than variations of grain size²¹.

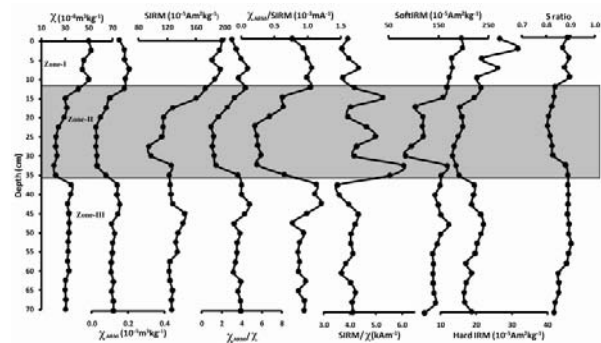


Fig. 4b—Vertical distribution of rock magnetic parameters in sediment core (C) from Coovum estuary.

Coercivity dependent parameters

Coercivity parameters such as Soft IRM, Hard IRM, S ratio and SIRM/χ are shown in Fig. 4a, b. The soft IRM parameter is a measure of concentration of low coercivity magnetic minerals (e.g. magnetite) while hard IRM reflects high coercivity magnetic minerals (e.g. hematite and goethite). The S ratio is a useful parameter for distinguishing magnetic mineral type, although it is also influenced by magnetic grain size. S ratio values closer to 1.0 indicate the preponderance of the soft (lower) coercive component (magnetite), whereas values closer to zero indicate the abundance of the hard (higher) coercive phase (hematite). SIRM/χ provides information on mineralogical variations (i.e., the relative proportions of magnetically hard and soft components) within the magnetic mineral sub fractions of sediments²². The changes in S ratio indicate that the zone I and III have preponderant of the soft magnetic minerals, whereas zone II shows dilution/ reduction of soft magnetic minerals with dia/para magnetic minerals. The mean values of mineral dependent parameters in tsunami deposits reflect the dilution of ferrimagnetic minerals with dia/paramagnetic minerals.

Statistical analysis

The correlation analysis of rock magnetic parameters versus all textural and geochemical and rock-magnetic parameters was carried out to study the connection and similarity between the different sedimentological units (Tables 1 and 2). The highly significant negative correlation of magnetic susceptibility with sand and positive correlation with silt and clay suggests that higher concentration of fine-grained ferrimagnetic minerals are associated with silt and clay particles than the sand content. The relationships among the magnetic minerals, geochemical and texture size of

Table 1—Correlation matrix for rock magnetic parameters versus texture size and geochemistry in Adayar estuary.

	χ	χ_{ARM}	SIRM	χ_{ARM}/χ	$\chi_{ARM}/SIRM$	SIRM/ χ	Soft IRM	Hard IRM	S-ratio
Sand	-0.89	-0.87	-0.82	0.77	-0.62	0.80	-0.59	-0.62	-0.71
Silt	0.84	0.83	0.78	-0.72	0.59	-0.76	0.59	0.52	0.75
Clay	0.86	0.91	0.84	-0.69	0.66	-0.78	0.63	0.65	0.66
SiO ₂	-0.72	-0.57	-0.52	0.68	-0.48	0.71	0.10	-0.12	-0.26
Al ₂ O ₃	0.79	0.55	0.67	-0.73	0.17	-0.60	0.13	0.13	0.40
Fe ₂ O ₃	0.85	0.89	0.87	-0.70	0.60	-0.78	0.67	0.56	0.79
CaO	0.88	0.72	0.74	-0.76	0.41	-0.73	0.29	0.27	0.49
MgO	0.87	0.70	0.73	-0.76	0.40	-0.72	0.27	0.25	0.48
K ₂ O	-0.76	-0.56	-0.60	0.70	-0.30	0.63	0.03	-0.04	-0.29
P ₂ O ₅	0.84	0.86	0.89	-0.69	0.51	-0.74	0.56	0.43	0.70
MnO	0.87	0.65	0.71	-0.80	0.32	-0.72	0.17	0.22	0.47

Table 2—Correlation matrix for rock magnetic parameters versus texture size and geochemistry in Coovum estuary.

	χ	χ_{ARM}	SIRM	χ_{ARM}/χ	$\chi_{ARM}/SIRM$	SIRM/ χ	Soft IRM	Hard IRM	S-ratio
Sand	-0.11	-0.36	0.00	-0.57	-0.58	0.22	-0.34	-0.22	-0.64
Silt	0.02	0.28	-0.09	0.51	0.52	-0.21	0.18	0.09	0.37
Clay	0.14	0.26	0.05	0.41	0.43	-0.21	0.25	0.12	0.37
SiO ₂	-0.20	-0.44	-0.02	-0.62	-0.66	0.46	-0.23	-0.29	-0.57
Al ₂ O ₃	0.72	0.78	0.59	0.73	0.77	-0.58	0.56	0.70	0.49
Fe ₂ O ₃	0.22	0.40	0.05	0.54	0.59	-0.43	0.23	0.28	0.51
CaO	0.14	0.39	-0.01	0.61	0.63	-0.40	0.22	0.28	0.55
MgO	0.25	0.47	0.08	0.63	0.67	-0.44	0.31	0.41	0.61
K ₂ O	-0.18	-0.44	0.01	-0.64	-0.67	0.41	-0.24	-0.21	-0.55
P ₂ O ₅	0.44	0.65	0.29	0.77	0.79	-0.44	0.49	0.48	0.72
MnO	0.44	0.46	0.29	0.45	0.50	-0.49	0.33	0.53	0.50

sediments in the zone II might be due to the erosion and transportation of sandy sediments by the tsunami wave; finer particles washed away induced deposits in onshore regions. Our study could give new perspectives in the tsunami research and for the development of innovative approaches, which could be tested and applied in several other Indian Ocean areas prone to tsunami hazard. These results also find applications in environmental risk management and shore protection measures.

Conclusions

Texture size variations, distribution pattern of geochemical elements and rock-magnetic studies in core sediments collected from Adayar and Coovum estuaries on the southeast coast of India were used to identify the depositional sequence in areas affected by the tsunami. The textural and geochemical results showed that the zone II sediment samples have more sand contents associated with the erosional / depositional features from the land/beach due to the high tsunami waves and intense current action that hit the coast. Rock magnetic data indicate that the tsunami-induced deposits are characterized by low magnetic susceptibility values linked to more

sand contents derived from high-energy waves. The correlation analysis infers that the erosion and transportation of sandy sediments from the tsunami waves have diluted the concentration of magnetic minerals or increased the dia/paramagnetic minerals and finer particles washed away. This work confirms that the rock magnetic techniques, being fast and cost effective, can be used as a proxy tool to identify the tsunami induced deposits along the coastal and estuarine regions.

Acknowledgements

We are thankful to the Director, Faculty of Marine Sciences, Annamalai University and Prof. N. Basavaiah, Indian Institute of Geomagnetism for providing all facilities. The NIO contribution number is 5490.

References

- 1 Kremer, K., G. Simpson, and S. Girardclos, Giant Lake Geneva tsunami in AD 563. *Nature Geoscience*, 2012.
- 2 Lay, T., H. Kanamori, C.J. Ammon, M. Nettles, S.N. Ward, R.C. Aster, S.L. Beck, S.L. Bilek, M.R. Brudzinski, and R. Butler, The great Sumatra-Andaman earthquake of 26 december 2004. *Science*, 2005. **308** (5725): p. 1127-1133.
- 3 Srinivasalu, S., N. Thangadurai, A.D. Switzer, V. Ram Mohan, and T. Ayyamperumal, Erosion and

- sedimentation in Kalpakkam (N Tamil Nadu, India) from the 26th December 2004 tsunami. *Marine Geology*, 2007. **240** (1): p. 65-75.
- 4 Kortekaas, S. and A. Dawson, Distinguishing tsunami and storm deposits: an example from Martinhal, SW Portugal. *Sedimentary Geology*, 2007. **200** (3): p. 208-221.
 - 5 Shanmugam, G., The tsunamite problem. *Journal of Sedimentary Research*, 2006. **76** (5): p. 718-730.
 - 6 Earnest, A., C. Rajendran, K. Rajendran, R. Anu, G. Arun, and P. Mohan, Near-field observations on the co-seismic deformation associated with the 26 December 2004 Andaman-Sumatra earthquake. *CURRENT SCIENCE-BANGALORE*, 2005. **89** (7): p. 1237.
 - 7 Kumaraguru, A., K. Jayakumar, J.J. Wilson, and C. Ramakritinan, Impact of the tsunami of 26 December 2004 on the coral reef environment of Gulf of Mannar and Palk Bay in the southeast coast of India. *Current Science*, 2005. **89** (10): p. 1729-1741.
 - 8 Nagendra, R., B.K. Kannan, C. Sajith, G. Sen, A. Reddy, and S. Srinivasalu, Nagappattinam coast, Tamil Nadu. *Current Science*, 2005. **89** (11): p. 1947.
 - 9 Altaff, K., J. Sugumaran, and S. Naveed, Impact of tsunami on meiofauna of Marina beach, Chennai, India. *Current Science*, 2005. **89** (1): p. 34-38.
 - 10 Srinivasalu, S., R. Nagendra, P. Rajalakshmi, N. Thangadurai, K. Arun Kumar, and H. Achyuthan, Geological signatures of M9 tsunami event on the sediments of Tamil Nadu Coast. *Tsunami: in the Indian content. Allied Publishers, India*, 2005: p. 171-181.
 - 11 Chaudhary, D., A. Ghosh, and J. Patolia, Characterization of soils in the tsunami-affected coastal areas of Tamil Nadu for agronomic rehabilitation. *Current Science*, 2006. **91** (1): p. 99-104.
 - 12 Mascarenhas, A., Extreme events, intrinsic landforms and humankind: post-tsunami scenario along Nagore-Velankanni coast, Tamil Nadu, India. *Current Science*, 2006. **90** (9): p. 1195-1201.
 - 13 Yeh, H., R. Chadha, M. Francis, T. Katada, G. Latha, C. Peterson, G. Raghuraman, and J. Singh, Tsunami runup survey along the southeast Indian coast. *Earthquake Spectra*, 2006. **22** (S3): p. 173-186.
 - 14 Anilkumar, N., Y. Sarma, K. Babu, M. Sudhakar, and P. Pandey, Post-tsunami oceanographic conditions in southern Arabian Sea and Bay of Bengal. *Current Science*, 2006. **90** (3): p. 421-427.
 - 15 Bahlburg, H. and R. Weiss, Sedimentology of the December 26, 2004, Sumatra tsunami deposits in eastern India (Tamil Nadu) and Kenya. *International Journal of Earth Sciences*, 2007. **96** (6): p. 1195-1209.
 - 16 Ingram, R., *Procedures in sedimentary petrology*, 1970: p. 49-67.
 - 17 Walden, J., J.P. Smith, and F. Oldfield, Environmental magnetism: A practical guide, Quaternary Research Association Technical Guide. 1999. **6**: p. 243.
 - 18 Peters, C. and M. Dekkers, Selected room temperature magnetic parameters as a function of mineralogy, concentration and grain size. *Physics and Chemistry of the Earth, Parts A/B/C*, 2003. **28** (16): p. 659-667.
 - 19 King, J., S.K. Banerjee, J. Marvin, and Ö. Özdemir, A comparison of different magnetic methods for determining the relative grain size of magnetite in natural materials: some results from lake sediments. *Earth and Planetary Science Letters*, 1982. **59** (2): p. 404-419.
 - 20 Maher, B.A., Magnetic properties of some synthetic sub-micron magnetites. *Geophysical Journal International*, 1988. **94** (1): p. 83-96.
 - 21 Font, E., C. Nascimento, R. Omira, M. Baptista, and P. Silva, Identification of tsunami-induced deposits using numerical modeling and rock magnetism techniques: A study case of the 1755 Lisbon tsunami in Algarve, Portugal. *Physics of the Earth and Planetary Interiors*, 2010. **182** (3): p. 187-198.
 - 22 Robinson, S., Early diagenesis in an organic-rich turbidite and pelagic clay sequence from the Cape Verde Abyssal Plain, NE Atlantic: magnetic and geochemical signals. *Sedimentary Geology*, 2001. **143** (1): p. 91-123.